Characterization of mechanical relaxation in a Cu-Zr-Al metallic glass

Chaoren Liu[a], Eloi Pineda[b], Daniel Crespo[a]

[a]Dept. Física Aplicada, EPSC, Universitat Politècnica Catalunya - BarcelonaTech, Esteve Terradas 5, 08860 Castelldefels, Spain.
chaorenliu@gmail.com / daniel.crespo@upc.edu

[b]Dept. Física i Enginyeria Nuclear, ESAB, Universitat Politècnica Catalunya - BarcelonaTech, Esteve Terradas 8, 08860 Castelldefels, Spain.
eloi.pineda@upc.edu

[*]Corresponding author:
Eloi Pineda
eloi.pineda@upc.edu
Tel. (34) 935 521 141

Abstract

The temperature dependence of the relaxation times of $Cu_{46}Zr_{46}Al_8$ glass was measured by means of mechanical spectroscopy and static stress-relaxation measurements. The weak intensity of secondary relaxation in this alloy allows us to correlate the characteristic times of dynamic and static measurements of primary relaxation. The glassy dynamics of an isoconfigurational state are found to follow an Adam-Gibbs-Vogel expression with the glassy state defined by a fictive temperature. The combination of both measurements proves that, in the frequency domain, the relaxation response can be well described by a single relaxation function above and below the glass transition. The change in relaxation times as function of the fictive temperature and the corresponding effects on the mechanical behavior are estimated and discussed.

Keywords: Amorphous alloys, Aging, Johari-Goldstein relaxation, Mechanical spectroscopy, Glass dynamics

1. Introduction

The structural dynamics of glasses is perceptible by probing different physical properties. In the liquid state, the characteristic times corresponding to different transport properties like viscosity, conductivity or diffusivity may show specific behaviors, but they all become strongly coupled near the glass transition. In the case of structural glasses, the relaxation of the structure is commonly explored applying static or oscillating electrical, mechanical or thermal stresses [1]. In many systems, the temperature dependence of the relaxation times above the glass transition temperature, T_g, can be described by a Vogel-Fulcher-Tammann (VFT) equation [2-5]

$$\tau_{VFT}(T) = \tau_0 \exp\left(\frac{B}{T - T_0}\right) \qquad \text{Eq.1}$$

where B and T_0 are empirical parameters characterizing the time dependence of a particular substance. The VFT function is usually not able to describe the liquid phase dynamics in the whole temperature range; the validity of Eq. 1 is in general restricted to a range of temperatures just above T_g.

The diverging slowing down of the liquid dynamics when $T \rightarrow T_0$ is stopped when the system becomes arrested in the non-equilibrium glassy state. At temperatures below glass transition, an equation proposed to describe the dynamics of the glassy state is [6]

$$\tau_{AGV}(T) = \tau_0 \exp\left[\frac{B}{T\left(1 - {T_0}/{T_f}\right)}\right] \qquad \text{Eq.2}$$

where T_f is the fictive temperature defined as the point where the glass behavior converges with the liquid. In this work we will call Eq. 2 as the Adam-Gibbs-Vogel (AGV) function [7]. Within the approach to glassy dynamics given by the AGV-function, T_f is the parameter defining the particular isoconfigurational glassy state achieved during the cooling process. Eq. 2 is equivalent to consider an Arrhenius behavior of the relaxation time with activation energy $E_{act}=RB/(1-T_0/T_f)$.

The non-equilibrium glassy phase is susceptible to change towards more stable configurations, this process is termed physical aging or structural relaxation and drives the glass to configurations with slower dynamics. Because of aging the relaxation times may change orders of magnitude [8,9], going from ~10^2 seconds to hundreds of hours or years depending on the temperature and the particular glassy state. The intrinsic relationship between the aging time and the relaxation time makes the time-evolving dynamics of glasses below T_g a complex non-linear problem [10]. Secondary or β-relaxations, faster than the main α-relaxation, are also a characteristic phenomenon of glassy systems. Usually, β-relaxations show an Arrhenius behavior below some departure point where they decouple from the main relaxation [11]. Although the presence of a secondary relaxation seems a universal feature of the glass transition, the microscopic origin, decoupling temperature, intensity and activation energy are unclear in many glassy substances.

In metallic glasses, the α-relaxation times are typically obtained from viscosity, calorimetric or mechanical spectroscopy measurements. Above T_g, the relaxation times are usually well described by a VFT behavior [12-16]. Below T_g, physical aging may change

the system state by annihilation of excess free volume [17] or other structural changes [18], while the dynamics of isoconfigurational glassy states follows Arrhenius behaviors [19,20]. Mechanical spectroscopy revealed the presence of β-relaxations in metallic glasses [21]. Some systems show a prominent β-relaxation peak [22,23], while other systems does not show an evident secondary relaxation but just a low-temperature excess wing of the main relaxation peak [24-27]. The presence of pronounced β-relaxations in metallic glasses has recently been associated to similar negative heats of mixing between the constituting elements of the alloy [28].

Interestingly, there is a link between the activation energy of relaxations below T_g and the initiation of mechanical flow events [29-31] and secondary relaxations are also considered the origin of physical aging or structural relaxation below T_g [32,33]. Physical aging and the corresponding change of fictive temperature may drive metallic glasses from ductile to brittle fracture behavior [34,35] or change chemical properties like the corrosion resistance [36]. The understanding of the relaxation spectrum of metallic glasses is then a key knowledge to control their properties and it has deep technological implications.

In this work we study the relaxation dynamics of $Cu_{46}Zr_{46}Al_8$ combining mechanical spectroscopy and static stress-relaxation tensile measurements. The response in mechanical spectroscopy is determined by a complex Young's modulus $E^*(\omega,T)=E'(\omega,T)+iE''(\omega,T)$. Micro alloying of Al in the Cu-Zr-Al system suppresses the low temperature shoulder of the α-relaxation peak and the relaxation below T_g is only perceived as an excess wing of the $E''(\omega,T)$ [28]. We will show that the full shape of the experimental $E''(T)$ can be understood considering a single Cole-Cole (CC) relaxation function

$$E^*(\omega,T) = E_0(T)\left[1 - \frac{1}{1+\left(i\omega\tau(T)\right)^{\alpha}}\right] \quad \text{Eq.3}$$

with $\tau(T)=\tau_{VFT}(T)$ and $\tau(T)=\tau_{AGV}(T)$ above and below T_g respectively. The α parameter in Eq. 3 characterizes the broadening of the relaxation peak. The validity of this model will be confirmed by means of static measurements of stress-relaxation, which give us direct access to the time domain response. We will also compare the relaxation response between as-quenched and relaxed glasses. We will show that the low-temperature, slow relaxations of $Cu_{46}Zr_{46}Al_8$ are described by the proposed VFT-AGV scheme if the glassy state do not suffer significant structural changes during the measurement. Finally, we will discuss the implications of the relaxation scheme proposed here on the mechanical properties of metallic glasses.

2. Materials and methods

Master alloy with a nominal composition of $Cu_{46}Zr_{46}Al_8$ was prepared by arc melting a mixture of constituent elements with a purity of above 99.9% under a Ti-gettered argon atmosphere. The master alloy was re-melted twice to ensure compositional homogeneity. The melt was quenched by injecting on a copper spinning wheel in a melt spinner device. The resulting ribbons had a thickness of 30±3 μm and a width of 1.5±0.2 mm. The amorphous character of the alloy was checked by XRD showing no signature of crystalline phases. The relaxed samples were prepared annealing 30 min at 693 K while applying a static stress in order to avoid the generation of residual stresses when cooling again the sample. Differential scanning calorimetry (DSC) was performed using a NETZSCH 404 F3 equipment on both as-quenched and relaxed samples. The DSC curves (Figure 1) show distinct shapes of the glass transition signal, with the expected overshooting in the relaxed

glass [37], while the crystallization at higher temperatures is not affected by the pre-annealing protocol as the memory of the system is lost once heated above the glass transition.

The tensile DMA measurements were performed on melt spun ribbons applying a heating rate of 1 K/min and frequencies between 0.1 and 50 Hz. The frequency response was obtained by applying oscillating tensile strains of 1μm amplitude on pieces of ribbon of about 10 mm length. Data was taken at temperature steps of 4 K from 500 K up to 750 K. The static stress-relaxation measurements were performed applying 'instantaneous' tensile deformations of amplitude $\varepsilon \sim 10^{-3}$, corresponding to an initial elastic stress of $\sigma_0 \sim 50–60$ MPa, and then measuring the stress decay during 1 hour. These measurements were performed in a Dynamo-Mechanical-Analyzer Q800 of TAinstruments.

The onset of glass transition is found at T_g=695 K when measured by DSC at 10 K/min. Therefore, the annealing protocol is expected to drive the system to a sufficient relaxed state as to avoid significant structural changes below ~690 K while heating at 1 K/min, thus ensuring the mechanical response $E^*(\omega,T)$ corresponds to an isoconfigurational glassy state.

3. Results

Figure 2 (top) shows the imaginary part of $E^*(\omega,T)$ of the relaxed ribbons as function of temperature for different frequencies. Figure 2 (bottom) shows $E''(\omega,T)$ measured at constant $\omega=2\pi$ s^{-1} in as-quenched and relaxed samples, showing the reduction of the excess wing by annealing. Following the same method as in ref. [38], the data sets obtained at each temperature were fitted to the CC-function of Eq.3. The value of $E_0(T)$ is taken constant

and equal to E_0=E'(T=500 K) and the two fitting parameters are then $\alpha(T)$ and $\tau(T)$. The fitting CC-functions at some selected temperatures are shown in the inset of figure 2 (top). For the relaxed samples, the values of $\alpha(T)$ show some dispersion around an average value α=0.35±0.06 with no clear tendency to increase or decrease with temperature. The inset of figure 1 (bottom) shows the E'' data points collected for all temperatures and frequencies as a function of $\omega\tau(T)$. Within the frequency and temperature window explored, the data is well described by a single peak with no observable change in the slope of the high-frequency wing, which would be indicative of a merged secondary process [39].

The $\tau(T)$ values obtained by fitting Eq. 3 to the experimental data are depicted in figure 3. The glass transition, defined as $\tau(T_g)=10^2$ s, is found at T_g=692 K. The change from equilibrium to non-equilibrium dynamics is also clearly seen, the solid lines correspond to VFT and AGV functions with parameters $\tau_0=6\times10^{-13}$ s, B=6220, T_0=512 K and T_f=694 K. The fragility parameter, calculated from the slope of the equilibrium curve at T_g, is found m=57. The glass transition temperature and the fragility correspond well with the expected for $Cu_{46}Zr_{46}Al_8$ glass [40]. As seen in the inset of figure 2 (top), at temperatures well below T_g the DMA data covers only a small part of the high frequency tail of the relaxation peak. Thus, an equally good description of data could be obtained with another relaxation function or a combination of two merged peaks.

In order to validate the measured $\tau(T)$ we performed static stress-relaxation measurements. Figure 4 shows the response at different temperatures, as well as the comparison between as-quenched and annealed samples. The time-evolving stress can be well modeled by a stretched exponential

$$\sigma(t) = \sigma_0 e^{-\left(\frac{t}{\tau}\right)^{\beta KWW}} \qquad \text{Eq.4}$$

where β_{KWW} is the Kohlrausch-Williams-Watts exponent. When transformed to frequency domain, Eq.4 corresponds to a relaxation peak with a high frequency tail following a power law similar to the one given by a CC-function with $\alpha \approx \beta_{KWW}$ [41]. Figure 3 shows that the values of τ(T) obtained from the static measurements are in good agreement with those obtained by DMA. The stretched exponent $\beta_{KWW}=0.4\pm0.1$ is similar to the values found in other metallic glasses [42] and it is slightly higher than the α parameter obtained for the CC-function. Here it should be noted that β_{KWW} shows a clear tendency to increase with temperature.

For the case of the as-quenched glass, the DMA measurements in the non-equilibrium region (T<700 K) do not correspond to a single isoconfigurational state. As the temperature rises the sample undergoes structural changes. In DMA measurements with tensile geometry this changes are readily observed by the increase of the storage modulus $E'(T)$ due to structural relaxation [32,38]. In order to model the relaxation response of the as-quenched samples by Eq. 3, we define two temperature regions: T<675 K and T>700 K. In the first region, we fix $E_0=E'_{aq}(T=500\ K)$, the storage modulus measured in the as-quenched samples before structural changes are detected. In the second region T>700 K, we fix $E_0=E'(T=500K)$ measured for the relaxed glass, which is 15% higher than $E'_{aq}(T=500\ K)$. The region between 675 and 700 K, where the system shows the more intense structural changes, is not fitted.

The $\tau(T)$ values obtained for the as-quenched ribbons are also shown in figure 3. The as-quenched glass coincides with the relaxed samples in the equilibrium region, while below T_g the relaxation times are more than one order of magnitude shorter. The broadening parameter of equation 3 is found to be $\alpha=0.39\pm0.06$. The as-quenched $\tau(T)$ points do not follow an AGV function with a constant T_f because of the in-situ structural changes taking place when heating at 1 K/min. Indeed, the relaxation times of the as-quenched samples can be interpreted as crossing isoconfigurational lines with decreasing T_f.

Figure 3 also shows $\tau(T)$ measured by static measurements of the as-quenched ribbons. The values of the stretching exponent show a tendency to increase with temperature, the average value is found $\beta_{KWW}=0.5\pm0.1$. It is worth to note that, despite the different experimental thermal protocols, the relaxation times are in full agreement with those obtained by DMA. The coincidence of the two methods indicates that between 500 K and 675 K a CC-function with an approximately constant E_0 and $\alpha=0.39\pm0.06$ is a good description of the frequency domain response of the as-quenched samples, at least within the temperature-frequency window probed. The values of α and β_{KWW} exponents did not show significant changes between as-quenched and relaxed samples and, contrary to what was observed in $Mg_{65}Cu_{25}Y_{10}$ alloy [38], the as-quenched samples do not show a significant change of the α parameter during the transition from non-equilibrium to equilibrium dynamics.

4. Discussion

Within the explored frequency and temperature windows, the above results show that the mechanical response of $Cu_{46}Zr_{46}Al_8$ can be modeled by a single α-relaxation and liquid and glassy dynamics given by the VFT and AGV functions. Similar to dielectric spectroscopy studies of other glassy substances, like inorganic or polymeric glasses, the CC-function is able to capture the characteristics of the relaxation in the frequency domain [41]. Here, it should be noted that the low frequency (high temperature) wing of the relaxation peak is not covered by this study. At 1 K/min the onset of crystallization is observed at T=745 K, inhibiting the access to the high-temperature wing. If the low frequency wing could be measured, it is possible that a complete Havriliak-Negami function with an asymmetry parameter $\gamma \neq 1$ would be necessary for describing the shape of the peak. However, the estimation of the $\tau(T)$ values and the exponential decay of the high-frequency wing (given by the α parameter of the CC-function) would not change significantly.

The results obtained here are consistent with those obtained for $Mg_{65}Cu_{25}Y_{10}$ [38], a metallic glass with a very different chemistry. In both cases, only a single relaxation process was necessary to understand the glass-liquid dynamics within the frequency and temperature window probed (f<100Hz). We must also note that the AGV function is a good description of the glass dynamics only if the glass is in an isoconfigurational state. Physical aging of metallic glasses has been recently studied by X-ray photon correlation spectroscopy (XPCS) in $Mg_{65}Cu_{25}Y_{10}$ and $Ni_{33}Zr_{67}$ glasses [8,43]. The complex aging behavior found in those works cannot be described by the simple VFT-AGV scheme proposed here. However, if the validity of the VFT-AGV description was verified in other

metallic glasses, it may give a useful tool to estimate the relaxation times and associated properties as function of the fictive temperature of the glass.

In other works, the low-temperature excess wing was modeled considering a β-process merged with the α-peak [25,32]. Although only the presence of the α relaxation is needed to explain the excess wing of $Cu_{46}Zr_{46}Al_8$, a secondary relaxation with very low intensity could be merged with the main loss peak. However, as in the case of $Mg_{65}Cu_{25}Y_{10}$ [44], the structural changes underwent by the as-quenched state during annealing at $T>0.8T_g$ can be associated to α-relaxation. As discussed above, the structural processes responsible of structural relaxation are linked with the fundamental deformation events originating plastic deformation of metallic glasses [30]. Therefore, in $Cu_{46}Zr_{46}Al_8$, these events could be associated to molecular rearrangements belonging to the broad peak of the α-relaxation. Let us now discuss the implications of such hypothesis.

Considering a well relaxed glass ($T_f \sim T_g$) and relaxation times following Eq.2, the average activation energy of structural relaxation below T_g would be determined as $E_{act}=RB/(1-T_0/T_g)$. Considering metallic glass systems with equilibrium dynamics above T_g determined by viscosity measurements and well described by a VFT behavior, the activation energy of the primary glass relaxation below T_g can be estimated from the B and T_0 parameters. This E_{act} is consistently well correlated with the W_{STZ}, the estimated work to activate a shear transformation zone [30,45], with E_{act} being 30-40% higher in most of the systems. Concerning to the effect of the fictive temperature, the ratio of activation energies of two isoconfigurational states would be $E_1/E_2=(1-T_0/T_{f1})/(1-T_0/T_{f2})$. For instance, in the $Cu_{46}Zr_{46}Al_8$ system of this work, an increase of 30K of the fictive temperature produces a 10% reduction of the activation energy for primary relaxation below T_g.

More significant than the changes in activation energy are the large changes in relaxation times between different glassy states. Let us consider that the system can sustain a maximum critical stress σ_c before inhomogeneous flow or fracture becomes activated. For deformation rates $\dot{\varepsilon} < \sigma_c / E\tau$ the glass is able to release stress via activation of primary relaxation rapidly enough to maintain the accumulated stress lower than σ_c. Therefore, the knowledge of the $\tau(T,T_f)$ behavior can give an estimation of the limiting values of $\dot{\varepsilon}$ at a given working temperature. For instance, considering $Cu_{46}Zr_{46}Al_8$ at 500 K, an increase of the fictive temperature of 5 K would double the limiting deformation rate.

5. Conclusions

A good description of liquid and glass dynamics is necessary to control processing conditions and physical properties of glasses. In this work, measurements of loss modulus and stress-relaxation times of $Cu_{46}Zr_{46}Al_8$ suggests that the relaxation behavior of this metallic glass can be well described by the VFT-AGV equations, at least within the frequency and temperature windows explored. Furthermore, the results presented here show that the low-temperature excess wing of internal loss is generated by the high-frequency tail of the α-relaxation, in contradiction to other glass-forming alloys where β-relaxation is considered the main mechanism driving structural changes below T_g. Further experimental work is needed to check the validity of this relaxation scheme in other metallic glass systems. This may confirm the relaxation scheme proposed here as a useful picture for understanding the effect of the relaxation state on the mechanical properties of metallic glasses.

Acknowledgments

C. Liu thanks the experimental assistance and the fruitful discussions with Mr. M. Madinehei and Dr. P. Bruna. This work was funded by CICYT Grant MAT2010-14907 and Generalitat de Catalunya Grants 2009SGR1251 and 2012FI-DGR.

Figure 1. DSC scans of the relaxed (black line) and as-quenched (red line) ribbons. The scans were performed at 10 K/min.

Figure 2. Top) Internal loss of the relaxed samples as function of temperature measured at 0.3, 3 and 30 Hz and 1 K/min. Top inset) Internal loss as function of frequency at different temperatures (symbols) and the corresponding fitted CC-functions (solid lines). Bottom) Internal loss peak measured at 1 Hz and 1 K/min. Comparison between relaxed (black symbols) and as-quenched (red symbols) ribbons. Bottom inset) Internal loss of the relaxed ribbons as a function of $\omega\tau(T)$.

Figure 3. Relaxation times calculated by DMA (open symbols) and static stress-relaxation measurements (full symbols). Relaxed samples (circles and diamonds) are compared with as-quenched ribbons (squares and triangles). Solid lines correspond to the VFT and AGV functions describing the $\tau(T)$ behavior of the relaxed samples. Dashed lines correspond to AGV functions with T_f=700, 710, 720, 730 and 740 K.

Figure 4. Relaxation of stress as function of time in static deformation measurements. Top) Measured stress at 673 K for relaxed (black diamonds) and as-quenched (red diamonds) ribbons. Solid lines correspond to the fitted stretched exponential decays. Bottom) Stress relaxation of the relaxed ribbons measured at 653, 663, 673, 683 and 693 K.

References

[1] C.A. Angell, K.L. Ngai, G.B. McKenna, P.F. McMillan, S.W. Martin, J. Appl. Phys. 88 (2000) 3113.

[2] H. Vogel, Phys. Physikalische Zeitschrift 22 (1921) 645.

[3] G.S. Fulcher, J. Am. Ceram. Soc. 8 (1925) 339.

[4] G.S. Fulcher, J. Am. Ceram. Soc. 8 (1925) 789.

[5] G. Tammann, W. Hesse, Zeitschrift fur Anorganische und Allgemeine Chemie 156 (1926) 245.

[6] R. Casalini, C.M. Roland, Phys. Rev. Lett. 102 (2009) 035701.

[7] I.M. HODGE, Macromolecules 20 (1987) 2897.

[8] B. Ruta, Y. Chushkin, G. Monaco, L. Cipelletti, E. Pineda, P. Bruna, V.M. Giordano, M. Gonzalez-Silveira, Phys. Rev. Lett. 109 (2012) 165701.

[9] B. Ruta, Y. Chushkin, G. Monaco, L. Cipelletti, V.M. Giordano, E. Pineda, P. Bruna, AIP Conf. Proc. 1518 (2013) 181–188.

[10] P. Lunkenheimer, R. Wehn, U. Schneider, A. Loidl, Phys. Rev. Lett. 95 (2005) 055702.

[11] G.P. Johari, M. Goldstein, J. Chem. Phys. 53 (1970) 2372.

[12] H.S. Chen, M. Goldstein, J. Appl. Phys. 43 (1972) 1642.

[13] H.S. Chen, J. Non. Cryst. Solids 27 (1978) 257.

[14] H.S. Chen, J. Non. Cryst. Solids 29 (1978) 223.

[15] R. Busch, W. Liu, W.L. Johnson, J. Appl. Phys. 83 (1998) 4134.

[16] G. Wilde, I.R. Lu, R. Willnecker, Mater. Sci. Eng. A 375 (2004) 417.

[17] A.R. Yavari, A. Le Moulec, A. Inoue, N. Nishiyama, N. Lupu, E. Matsubara, W.J. Botta, G. Vaughan, M. Di Michiel, A. Kvick, Acta Mater. 53 (2005) 1611.

[18] B. Ruta, V.M. Giordano, L. Erra, C. Liu, E. Pineda, J. Alloys Compd. (2013) Accepted. URL: 10.1016/j.jallcom.2013.12.162.

[19] A.I. Taub, F. Spaepen, Acta Metall. 28 (1980) 1781.

[20] M.L. Lind, G. Duan, W.L. Johnson, Phys. Rev. Lett. 97 (2006) 015501.

[21] H.-B. Yu, W.-H. Wang, K. Samwer, Mater. TODAY 16 (2013) 183.

[22] Z. Wang, H.B. Yu, P. Wen, H.Y. Bai, W.H. Wang, J. Physics-Condensed Matter 23 (2011) 142202.

[23] J.C. Qiao, J.M. Pelletier, J. Appl. Phys. 112 (2012) 083528.

[24] P. Rosner, K. Samwer, P. Lunkenheimer, Europhys. Lett. 68 (2004) 226.

[25] K.L. Ngai, J. Non. Cryst. Solids 352 (2006) 404.

[26] J. Hachenberg, K. Samwer, J. Non. Cryst. Solids 352 (2006) 5110.

[27] Z.F. Zhao, P. Wen, C.H. Shek, W.H. Wang, Phys. Rev. B 75 (2007) 174201.

[28] H. Bin Yu, K. Samwer, W.H. Wang, H.Y. Bai, Nat. Commun. 4 (2013) 2204.

[29] H.B. Yu, W.H. Wang, H.Y. Bai, Y. Wu, M.W. Chen, Phys. Rev. B 81 (2010) 220201.

[30] W.H. Wang, J. Appl. Phys. 110 (2011) 053521.

[31] H.B. Yu, X. Shen, Z. Wang, L. Gu, W.H. Wang, H.Y. Bai, Phys. Rev. Lett. 108 (2012) 015504.

[32] J. Hachenberg, D. Bedorf, K. Samwer, R. Richert, A. Kahl, M.D. Demetriou, W.L. Johnson, Appl. Phys. Lett. 92 (2008) 131911.

[33] L. Hu, Y. Yue, J. Phys. Chem. C 113 (2009) 15001.

[34] J.J. Lewandowski, W.H. Wang, A.L. Greer, Philos. Mag. Lett. 85 (2005) 77.

[35] G. Kumar, P. Neibecker, Y.H. Liu, J. Schroers, Nat. Commun. 4 (2013) 1536.

[36] M.J. Duarte, J. Klemm, S.O. Klemm, K.J.J. Mayrhofer, M. Stratmann, S. Borodin, A.H. Romero, M. Madinehei, D. Crespo, J. Serrano, S.S.A. Gerstl, P.P. Choi, D. Raabe, F.U. Renner, Science 341 (2013) 372.

[37] O. V Mazurin, Glas. Phys. Chem. 33 (2007) 22.

[38] E. Pineda, P. Bruna, B. Ruta, M. Gonzalez-Silveira, D. Crespo, Acta Mater. 61 (2013) 3002.

[39] T. Bauer, P. Lunkenheimer, S. Kastner, A. Loidl, Phys. Rev. Lett. 110 (2013) 107603.

[40] S. Pauly, J. Das, N. Mattern, D.H. Kim, J. Eckert, Intermetallics 17 (2009) 453.

[41] C. Svanberg, J. Appl. Phys. 94 (2003) 4191.

[42] L.-M. Wang, R. Liu, W.H. Wang, J. Chem. Phys. 128 (2008) 164503.

[43] B. Ruta, G. Baldi, G. Monaco, Y. Chushkin, J. Chem. Phys. 138 (2013) 054508.

[44] F. Zhai, E. Pineda, B. Ruta, M. Gonzalez-Silveira, D. Crespo, J. Alloys Compd. (2013) Accepted. URL:10.1016/j.jallcom.2013.11.120.

[45] W.L. Johnson, K. Samwer, Phys. Rev. Lett. 95 (2005) 195501.

Highlights:

1. Mechanical relaxation dynamics of a Cu-Zr-Al metallic glass fully characterized
2. Mechanical spectroscopy combined with static stress-relaxation measurements
3. Alpha-relaxation process described by a Cole-Cole function
4. Relaxation times following Arrhenius and Vogel-Fulcher-Tammann behaviors
5. Mechanical relaxation described without the presence of a secondary relaxation

Figure1

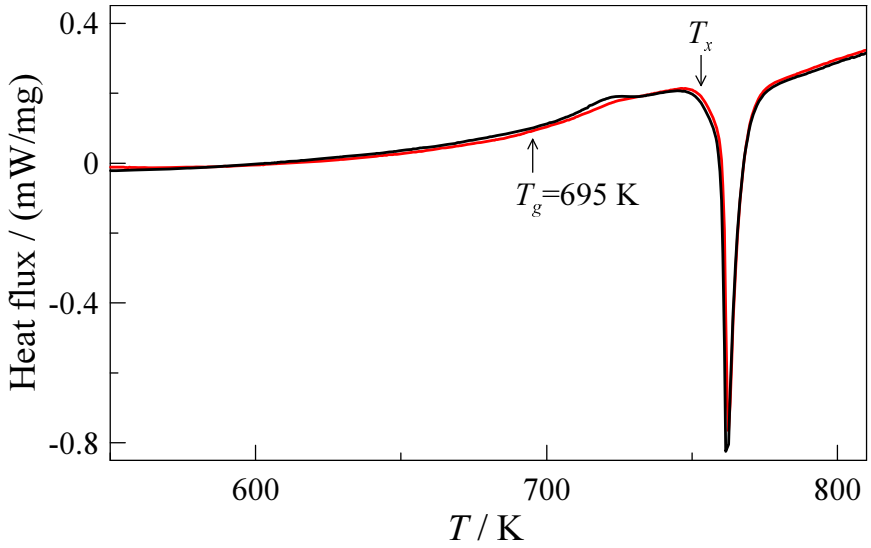

Figure 1

Figure2

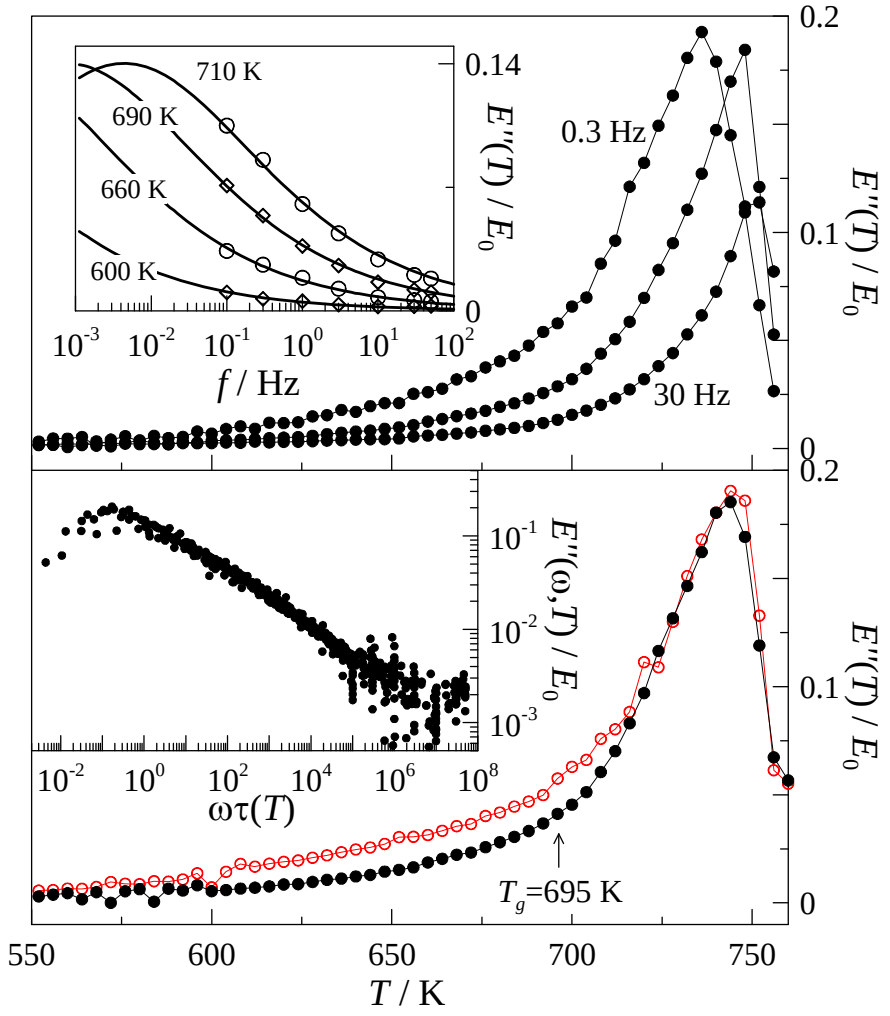

Figure 1

Figure3

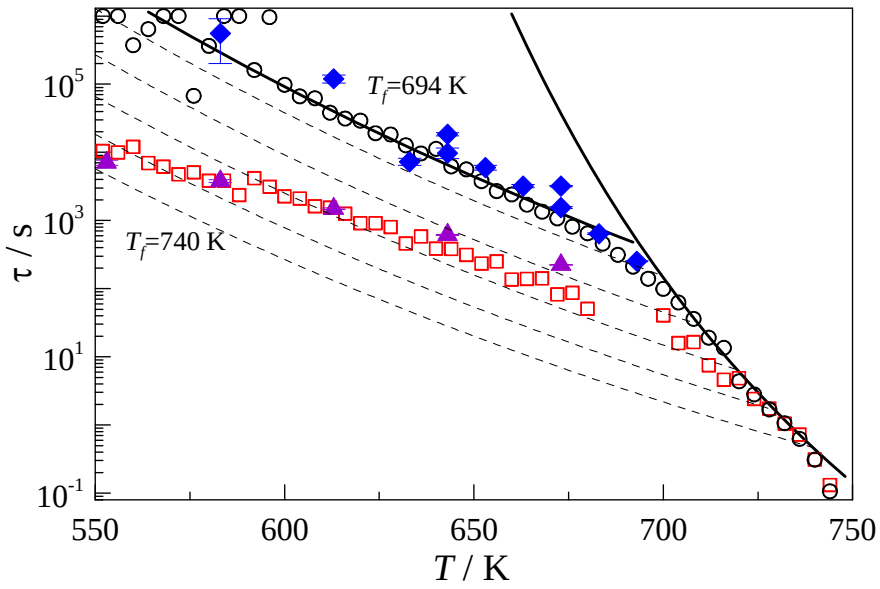

Figure 2

Figure4

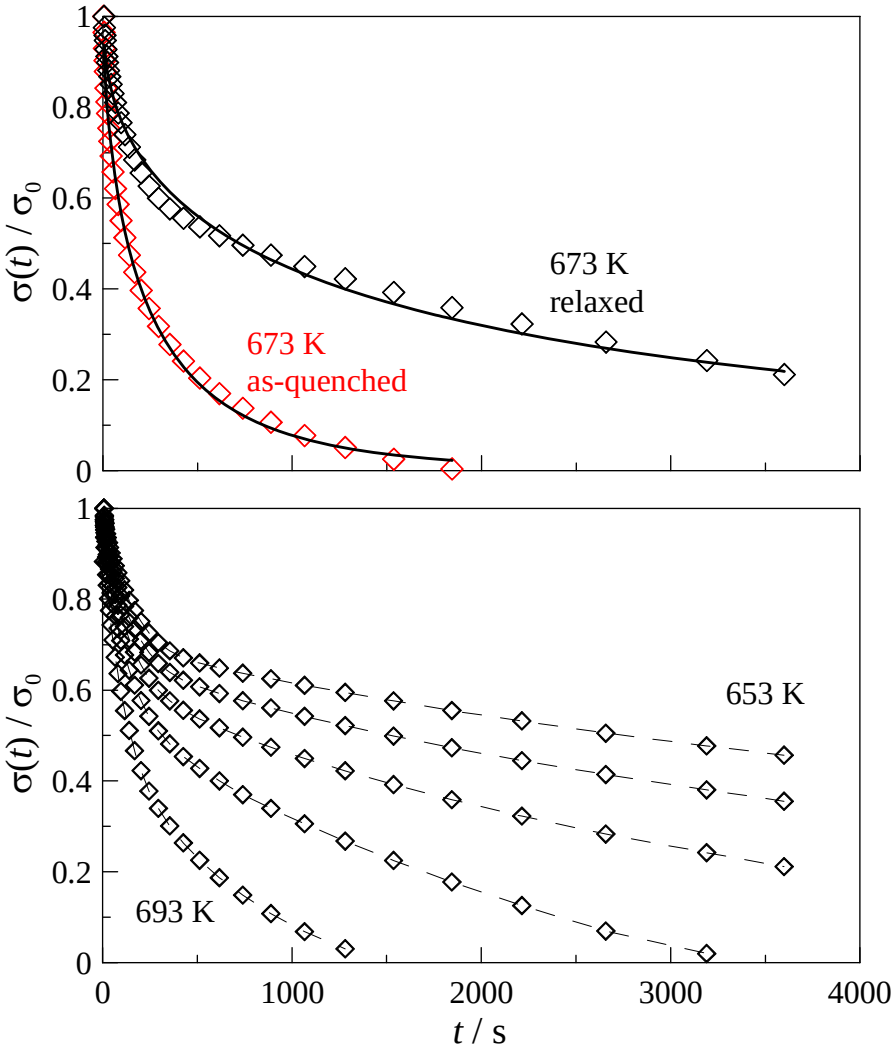

Figure 3